BDDC PRECONDITIONERS FOR VIRTUAL ELEMENT APPROXIMATIONS OF THE THREE-DIMENSIONAL STOKES EQUATIONS*

TOMMASO BEVILACQUA†, FRANCO DASSI‡, STEFANO ZAMPINI§, AND SIMONE SCACCHI¶

Abstract. The Virtual Element Method (VEM) is a novel family of numerical methods for approximating partial differential equations on general polygonal or polyhedral computational grids. This work aims to propose a Balancing Domain Decomposition by Constraints (BDDC) preconditioner that allows using the conjugate gradient method to compute the solution of the saddle-point linear systems arising from the VEM discretization of the three-dimensional Stokes equations. We prove the scalability and quasi-optimality of the algorithm and confirm the theoretical findings with parallel computations. Numerical results with adaptively generated coarse spaces confirm the method's robustness in the presence of large jumps in the viscosity and with high-order VEM discretizations.

Key words. Virtual element method, Divergence free discretization, Saddle-point linear system, Domain decomposition preconditioner

AMS subject classifications. 68Q25, 68R10, 68U05

1. Introduction.

The Virtual Element Method (VEM, [10]) is a recent technology for the numerical approximation of Partial Differential Equations (PDEs) which can deal with computational grids of very general polygonal/polyhedral shape. Effective VEM discretizations have been developed for several PDEs; the interested reader should consult the recent special issue [9] and the book [5] for further details. Regarding computational fluid dynamics, divergence-free VEM discretizations of the Stokes and Navier-Stokes equations have been proposed in [12, 13, 11].

Due to the arbitrary shape of polytopal elements, the linear systems arising from VEM discretizations of PDEs are generally worse conditioned than in case of Finite Element Methods (FEM). Some recent studies have proposed multigrid and domain decomposition preconditioners for scalar elliptic equations in primal form: see [6, 7] for a multigrid preconditioner, [14, 15, 29, 30] for Balancing Domain Decomposition by Constraints (BDDC) and Dual-Primal Finite Element Tearing and Interconnecting (FETI-DP) preconditioners, and [20, 21] for Overlapping Additive Schwarz preconditioners.

A few works have investigated the efficient solution of VEM approximations for saddle point problems. In [24, 23] parallel block algebraic multigrid preconditioners have been proposed for three-dimensional VEM approximations of elliptic, Stokes, and Maxwell equations in mixed form. BDDC preconditioners for three-dimensional scalar elliptic equations in mixed form have been constructed and analyzed in [25]. BDDC methods for two-dimensional VEM discretizations of the Stokes equations have been studied in [17].

The present study aims to construct, analyze and numerically validate a BDDC preconditioner for three-dimensional divergence-free VEM discretizations of the Stokes

*Submitted to the editors DATE.

Funding: This work was funded by the Fog Research Institute under contract no. FRI-454.

†University of Milan, (tommaso.bevilacqua@unimi.it).

‡University of Milano-Bicocca (franco.dassi@unimib.it.

§King Abdullah University of Science and Tecnology, (stefano.zampini@kaust.edu.sa).

¶University of Milan, (simone.scacchi@unimi.it).

equations. The novelty with respect to our previous work [17] is the extension of both analysis and implementation to the three-dimensional case, the inclusion of deluxe scaling functions to average the dual unknowns after local solves, the development of an adaptive technique to enrich the coarse space, and the parallel implementation of the algorithm. From the theoretical point of view, we prove the scalability and quasi-optimality of the method in the case of a homogeneous fluid with constant viscosity. We validate the theoretical estimates with several parallel numerical tests, and we provide numerical evidence for the robustness of the preconditioner with respect to the degree of approximation and the shape of the polyhedral elements. Finally, we compare the proposed algorithm with other parallel solvers in terms of computational efficiency, and we confirm the robustness of our approach on a challenging multi-sinker test case with heterogeneous viscosity [35].

2. Continuous problem: the Stokes equations. We follow the standard notation for the Sobolev spaces as in [1]. Moreover we recall the differential operators: the vector Laplacian $\boldsymbol{\Delta}$, the divergence div, the gradient ∇ and the strain tensor $\varepsilon_{ij}(\mathbf{u}) := \frac{1}{2}\big(\frac{\partial u_i}{\partial x_j} + \frac{\partial u_j}{\partial x_i}\big)$.
We denote with $\mathcal{O}$ a generic geometrical entity (element, face, edge) having diameter $h_{\mathcal{O}}$ and we introduce for any $\mathcal{O}$ and $n \in \mathbb{N}$ the spaces:

- $\mathbb{P}_n(\mathcal{O})$ the set of polynomials on $\mathcal{O}$ of degree $\leq n$ (with $\mathbb{P}_{-1}(\mathcal{O}) := \{0\}$),
- $\widehat{\mathbb{P}}_{n\setminus m}(\mathcal{O}) := \mathbb{P}_n(\mathcal{O}) \setminus \mathbb{P}_m(\mathcal{O})$ for $n > m$, denotes the space of polynomials in $\mathbb{P}_n(\mathcal{O})$ with monomials of degree strictly greater than m.

Let $\Omega \subseteq \mathbb{R}^3$ be a bounded Lipschitz domain, with $\Gamma = \partial\Omega$, and consider the stationary Stokes problem on Ω with homogeneous Dirichlet boundary conditions:

$$\begin{cases} \text{Find } (\mathbf{u}, p) \text{ such that} & \\ -\nu\boldsymbol{\Delta}\mathbf{u} - \nabla p = \mathbf{f} & \text{in } \Omega \\ \operatorname{div}\mathbf{u} = 0 & \text{in } \Omega \\ \mathbf{u} = 0 & \text{on } \Gamma, \end{cases} \tag{2.1}$$

where $\mathbf{u}$ and p are respectively the velocity and the pressure fields, $\mathbf{f} \in [H^{-1}(\Omega)]^3$ represents the external force and $\nu \in \mathbb{R}, \nu > 0$ is the viscosity, assumed constant for the purposes of our analysis. Numerical evidence for the robustness of the algorithm in the presence of highly heterogenous viscosity is provided in Section 8.

Let us consider the spaces:

$$\mathbf{V} := [H_0^1(\Omega)]^3, \qquad Q := L_0^2(\Omega) = \left\{ q \in L^2(\Omega) \quad s.t. \quad \int_\Omega q \, \mathrm{d}\Omega = 0 \right\}. \tag{2.2}$$

Let the bilinear forms $a(\cdot,\cdot) : \mathbf{V} \times \mathbf{V} \to \mathbb{R}$ and $b : \mathbf{V} \times Q \to \mathbb{R}$ be defined as:

$$a(\mathbf{u}, \mathbf{v}) := \int_\Omega \nu\varepsilon(\mathbf{u}) : \varepsilon(\mathbf{v}) \, \mathrm{d}\Omega \qquad \text{for all } \mathbf{u}, \mathbf{v} \in \mathbf{V} \tag{2.3}$$

$$b(\mathbf{v}, q) := \int_\Omega \operatorname{div}\mathbf{v} \, q \, \mathrm{d}\Omega \qquad \text{for all } \mathbf{u} \in \mathbf{V}, q \in Q. \tag{2.4}$$

Then a standard variational formulation of problem (2.1) reads:

$$\begin{cases} \text{find } (\mathbf{u}, p) \in \mathbf{V} \times Q \text{ such that} & \\ a(\mathbf{u}, \mathbf{v}) + b(\mathbf{v}, p) = (\mathbf{f}, \mathbf{v}) & \text{for all } \mathbf{v} \in \mathbf{V}, \\ b(\mathbf{u}, q) = 0 & \text{for all } q \in Q, \end{cases} \tag{2.5}$$

where

$$(\mathbf{f},\mathbf{v}) := \int_\Omega \mathbf{f}\cdot\mathbf{v}\ \mathrm{d}\Omega.$$

We refer to [18] for the mathematical analysis of this problem.

We recall here two lemmas (see [31] Section 2) that we will need in Section 4: the first one states the equivalence between the Stokes and elasticity bilinear forms and their H^1 seminorms, while the second one is a Korn-type inequality.

LEMMA 2.1. *There exists a constant $c>0$ such that:*

$$c\|\nabla\mathbf{u}\|_{[L^2(\Omega)]} \le \|\varepsilon(\mathbf{u})\|_{[L^2(\Omega)]} \le \|\nabla\mathbf{u}\|_{[L^2(\Omega)]} \qquad \forall \mathbf{u}\in[H^1(\Omega)]^3, \mathbf{u}\perp ker(\varepsilon),$$

where $ker(\varepsilon)$ is the space of the rigid body modes of the elasticity problem.

LEMMA 2.2. *Let $\Omega\subset\mathbb{R}^3$ be a Lipschitz domain of diameter H and $\Sigma\subset\partial\Omega$ be an open subset with positive surface measure. There exists a positive constant C, independent of H such that:*

$$\inf_{\mathbf{r}\in ker(\varepsilon)} \|\mathbf{u}-\mathbf{r}\|^2_{L^2(\Omega)} \le CH|\mathbf{u}|_{E(\Sigma)} \qquad \forall \mathbf{u}\in[H^{1/2}(\Sigma)]^3,$$

where $|\mathbf{u}|_{E(\Sigma)} := \inf_{\mathbf{v}\in[H^1(\Omega)]^3,\mathbf{v}_{|\Sigma}=\mathbf{u}} \|\varepsilon(\mathbf{v})\|_{L^2(\Omega)}$.

3. Virtual element discretization. We present here the discretization of problem (2.1), based on the virtual element space introduced in Section 3 of [11], that is designed to solve a Stokes-like problem element-wise.

Mesh construction. Let $\{\mathcal{T}_h\}_h$ be a sequence of decompositions of Ω into general shape-regular polyhedral elements K (in the sense of Definition 2.1 of [15]) with a mesh size:

$$h := \sup_{K\in\mathcal{T}_h} h_K,$$

where h_K is the diameter of K.

We suppose that, for all h, each element $K\in\mathcal{T}_h$ satisfies the following assumptions:

- (**A1**) K is star-shaped with respect to a ball B_K of radius $\ge \gamma h_K$,
- (**A2**) every face f of K is star-shaped with respect to a disk B_f of radius $\ge \gamma\, h_K$,
- (**A3**) every edge e of K satisfies $h_e \ge \gamma h_K$,

where γ is a uniform positive constant. These hypotheses could be weakened as in [10], for example, by assuming that every K is a union of a finite (and uniformly bounded) number of star-shaped domains, each satisfying (**A1**).

We denote with N_K, N_V, N_f and N_e the total number of polyhedra, vertices, faces, and edges of the decomposition $\mathcal{T}_h$, respectively.

Since we are interested in estimates with a dependence on the number and size of the subdomains and polyhedral elements, we will denote with the symbol $\lesssim$ a bound up to a generic positive constant that is independent of the previous quantities, but which may depend on Ω, on the polynomial order k and the constant γ of Assumptions (**A1**) – (**A3**).

Before introducing the discrete velocity and pressure spaces, we define some suitable projection operators that will be directly computable with the degrees of freedom (dofs). For any $n\in\mathbb{N}$ and each geometric entity $\mathcal{O}$ (element or face), we introduce the following polynomial projections:

- the L^2-*projection* $\Pi_n^{0,\mathcal{O}} : L^2(\mathcal{O}) \to \mathbb{P}_n(\mathcal{O})$, defined for any $v \in L^2(\mathcal{O})$ by:

$$\int_{\mathcal{O}} q_n(v - \Pi_n^{0,\mathcal{O}} v)\, \mathrm{d}\mathcal{O} = 0 \qquad \text{for all } q_n \in \mathbb{P}_n(\mathcal{O}), \tag{3.1}$$

  with obvious extension for vector functions $\Pi_n^{0,\mathcal{O}} : [L^2(\mathcal{O})]^3 \to [\mathbb{P}_n(\mathcal{O})]^3$ and tensor functions $\Pi_n^{0,\mathcal{O}} : [L^2(\mathcal{O})]^{3\times 3} \to [\mathbb{P}_n(\mathcal{O})]^{3\times 3}$,
- the H^1-*seminorm projection* $\Pi_n^{\nabla,\mathcal{O}} : H^1(\mathcal{O}) \to \mathbb{P}_n(\mathcal{O})$, defined for any $v \in H^1(\mathcal{O})$ by:

$$\begin{cases} \displaystyle\int_{\mathcal{O}} \nabla q_n \cdot \nabla(v - \Pi_n^{\nabla,\mathcal{O}} v)\, \mathrm{d}\mathcal{O} = 0 \qquad \text{for all } q_n \in \mathbb{P}_n(\mathcal{O}), \\ \displaystyle\int_{\partial\mathcal{O}} (v - \Pi_n^{\nabla,\mathcal{O}} v)\, \mathrm{d}\sigma = 0, \end{cases} \tag{3.2}$$

  with obvious extension for vector functions $\Pi_n^{\nabla,\mathcal{O}} : [H^1(\mathcal{O})]^3 \to [\mathbb{P}_n(\mathcal{O})]^3$.

Pressure space. We start by constructing the discrete space Q_h. This is a natural extension of the two-dimensional space [12] and, following [11], we define:

$$Q_h^K := \mathbb{P}_{k-1}(K), \tag{3.3}$$

therefore the corresponding dofs are chosen defining for each $q \in Q_h^K$ the following linear operator:

- $\mathbf{D_Q}$: the moments up to order $k-1$ of q:

$$\int_K q p_{k-1}\, \mathrm{d}K \qquad \text{for any } p_{k-1} \in \mathbb{P}_{k-1}(K).$$

The global space is given by:

$$Q_h := \{q \in L^2(\Omega) \quad \text{s.t.} \quad q_{|K} \in Q_h^K \quad \text{for all } K \in \mathcal{T}_h\}. \tag{3.4}$$

Velocity space. The space $\mathbf{V}_h$, as defined in [11], is the three-dimensional extension of the two-dimensional velocity space introduced in [12], where the extensive use of the enhancement technique [2] is needed to achieve the computability of suitable polynomial projection operators. We start by considering each face f of a polyhedral element K, then we define:

$$\begin{aligned} \widehat{\mathbb{B}}_k(f) := \{v \in & H^1(f) \text{ s.t. (i) } v_{|\partial f} \in C^0(\partial f), v_{|e} \in \mathbb{P}_k(e) \text{ for all } e \in \partial f, \\ & \text{(ii) } \Delta_f v \in \mathbb{P}_{k+1}(f), \\ & \text{(iii) } (v - \Pi_k^{\nabla,f} v, \widehat{p}_{k+1})_f = 0 \text{ for all } \widehat{p}_{k+1} \in \widehat{\mathbb{P}}_{k+1\setminus k-2}(f)\} \end{aligned} \tag{3.5}$$

and the boundary space:

$$\widehat{\mathbb{B}}_k(\partial K) := \{v \in C^0(\partial K) \text{ s.t. } v_{|f} \in \widehat{\mathbb{B}}_k(f) \text{ for any } f \in \partial K\}. \tag{3.6}$$

Then on the polyhedron K we first define the virtual element space:

$$\begin{aligned} \widetilde{\mathbf{V}}_h^K := \{\mathbf{v} \in & [H^1(K)]^3 \text{ s.t. (i) } \mathbf{v}_{|\partial K} \in [\widehat{\mathbb{B}}_k(\partial K)]^3, \\ & \text{(ii) } \Delta\mathbf{v} + \nabla s \in \mathbf{x} \wedge [\mathbb{P}_{k-1}(K)]^3 \text{ for some } s \in L_0^2(K), \\ & \text{(iii) } \operatorname{div}\mathbf{v} \in \mathbb{P}_{k-1}(K)\}, \end{aligned} \tag{3.7}$$

being $\mathbf{x} = (x_1, x_2, x_3)$ the independent variables, and $\wedge$ the cross product. The velocity space is then defined as:

$$\mathbf{V}_h^K := \{\mathbf{v} \in \widetilde{\mathbf{V}}_h^K \text{ s.t. } (\mathbf{v} - \Pi_k^{\nabla,K}\mathbf{v}, \mathbf{x} \wedge \widehat{\mathbf{p}}_{k-1})_K = 0 \quad \forall \widehat{\mathbf{p}}_{k-1} \in [\widehat{\mathbb{P}}_{k-1\setminus k-3}(K)]^3\}. \tag{3.8}$$

Remark 3.1. The "super-enhanced" constraints (iii) in (3.5) and in (3.8) are necessary to achieve the computability of the polynomial projection operators $\Pi_{k+1}^{0,f}$ and $\Pi_k^{0,K}$ (see Proposition 5.1 in [11]).

Remark 3.2. Note that the approximation property is guaranteed by the fact that the spaces $\mathbf{V}_h^K$ and Q_h^K contain $[\mathbb{P}_k(K)]^3$ and $\mathbb{P}_{k-1}(K)$, respectively.

Given $\mathbf{v} \in \mathbf{V}_h^K$, the dofs of the local velocity space $\mathbf{V}_h^K$ are defined by means of the following set of linear operators:

- $\mathbf{D}_\mathbf{V}^\mathbf{1}$: the values of $\mathbf{v}$ at the vertices of K;
- $\mathbf{D}_\mathbf{V}^\mathbf{2}$: the values of $\mathbf{v}$ at $k-1$ distinct points of every edge e of K;
- $\mathbf{D}_\mathbf{V}^\mathbf{3}$: the face moments of $\mathbf{v}$ (split into normal and tangential components):

$$\int_f (\mathbf{v} \cdot \mathbf{n}_K^f) p_{k-2} \, \mathrm{d}f, \quad \int_f \mathbf{v}_\tau \cdot \mathbf{p}_{k-2} \, \mathrm{d}f, \tag{3.9}$$

  for all $p_{k-2} \in \mathbb{P}_{k-2}(f)$ and $\mathbf{p}_{k-2} \in [\mathbb{P}_{k-2}(f)]^2$, where $\mathbf{n}_K^f$ is the normal vector associated to the face f and $\mathbf{v}_\tau$ is the 2D vector field defined on ∂K, s.t. on each face $f \in \partial K$:

$$\mathbf{v}_\tau := \mathbf{v} - (\mathbf{v} \cdot \mathbf{n}_K^f)\mathbf{n}_K^f;$$

- $\mathbf{D}_\mathbf{V}^\mathbf{4}$: the volume moments of $\mathbf{v}$:

$$\int_K \mathbf{v} \cdot (\mathbf{x} \wedge \mathbf{p}_{k-3}) \, \mathrm{d}K \qquad \text{for all } \mathbf{p}_{k-3} \in [\mathbb{P}_{k-3}(K)]^3; \tag{3.10}$$

- $\mathbf{D}_\mathbf{V}^\mathbf{5}$: the volume moments of $\operatorname{div} \mathbf{v}$:

$$\int_K \operatorname{div} \mathbf{v} \, \widehat{p}_{k-1} \, \mathrm{d}K \qquad \text{for all } \widehat{p}_{k-1} \in \widehat{\mathbb{P}}_{k-1\setminus 0}(K). \tag{3.11}$$

The global space $\mathbf{V}_h$ is obtained by gluing the local spaces:

$$\mathbf{V}_h := \{\mathbf{v} \in [H^1(\Omega)]^3 \text{ s.t. } \mathbf{v}_{|K} \in \mathbf{V}_h^K \text{ for all } K \in \mathcal{T}_h\}. \tag{3.12}$$

3.1. Discrete bilinear forms and load term approximation. We first decompose the bilinear forms $a(\cdot,\cdot)$ and $b(\cdot,\cdot)$, and the load term $\mathbf{f}$ defined in (2.5) into local contributions:

$$a(\mathbf{u},\mathbf{v}) := \sum_{K\in\mathcal{T}_h} a^K(\mathbf{u},\mathbf{v}), \quad b(\mathbf{v},p) := \sum_{K\in\mathcal{T}_h} b^K(\mathbf{v},p), \quad (\mathbf{f},\mathbf{v}) := \sum_{K\in\mathcal{T}_h} (\mathbf{f},\mathbf{v})_K, \tag{3.13}$$

for all $\mathbf{u}, \mathbf{v} \in [H^1(\Omega)]^3$ and $p \in Q_h$.

We note that we do not need any approximation for the divergence bilinear form since we can compute exactly $b(\mathbf{v}_h, q_h)$ for all $\mathbf{v}_h \in \mathbf{V}_h$ and $q_h \in Q_h$ directly form the $\mathbf{D}_\mathbf{V}^\mathbf{1}, \mathbf{D}_\mathbf{V}^\mathbf{2}$ and $\mathbf{D}_\mathbf{V}^\mathbf{5}$.

Instead, the bilinear form $a(\cdot,\cdot)$ is not directly computable from the dofs when both entries are "virtual". Following [11], we define the approximation:

$$a_h^K(\mathbf{u},\mathbf{v}) := \int_K (\Pi_{k-1}^{0,K}\varepsilon(\mathbf{u})) : (\Pi_{k-1}^{0,K}\varepsilon(\mathbf{v}))\ \mathrm{d}K + S^K((I-\Pi_k^{\nabla,K})\mathbf{u},(I-\Pi_k^{\nabla,K})\mathbf{v}), \tag{3.14}$$

for all $\mathbf{u},\mathbf{v}\in\mathbf{V}_h^K$, where:

$$\Pi_{k-1}^{0,K}\varepsilon(\mathbf{u}) = \frac{\Pi_{k-1}^{0,K}\nabla\mathbf{u} + (\Pi_{k-1}^{0,K}\nabla\mathbf{u})^T}{2}.$$

The approximate bilinear form (3.14) is obtained as the sum of two contributions, the first term known as the consistency part and the second term known as the stabilization part, where $S^P : \mathbf{V}_h^K\times\mathbf{V}_h^K\to\mathbb{R}$ is a suitable symmetric bilinear form that has to scale like the H^1-seminorm.

Remark 3.3. For the numerical experiments in Section 8, we use the D-recipe stabilization introduced in Section 6 of [11].

The load term is approximated by taking:

$$(\mathbf{f}_h,\mathbf{v})_K := \int_K \Pi_k^{0,K} f\cdot\mathbf{v}\ \mathrm{d}K. \tag{3.15}$$

Finally, the global forms are obtained by simply gluing elements' contributions:

$$a_h(\mathbf{u},\mathbf{v}) := \sum_{K\in\mathcal{T}_h} a_h^K(\mathbf{u},\mathbf{v}), \quad (\mathbf{f}_h,\mathbf{v}) := \sum_{K\in\mathcal{T}_h}(\mathbf{f}_h,\mathbf{v})_K, \tag{3.16}$$

for all $\mathbf{u},\mathbf{v}\in\mathbf{V}_h$.

3.2. Discrete problem. Using the discrete spaces (3.12) and (3.4) and the discrete linear and bilinear forms previously introduced, the discrete Stokes problem reads as follows:

$$\begin{cases} \text{find } (\mathbf{u}_h,p_h)\in\mathbf{V}_{h,0}\times Q_{h,0} \text{ such that} & \\ a_h(\mathbf{u}_h,\mathbf{v}_h)+b(\mathbf{v}_h,p_h) = (\mathbf{f}_h,\mathbf{v}_h) & \text{for all } \mathbf{v}_h\in\mathbf{V}_{h,0},\\ b(\mathbf{u}_h,q_h) = 0 & \text{for all } q_h\in Q_{h,0}, \end{cases} \tag{3.17}$$

where $\mathbf{V}_{h,0} := \mathbf{V}_h\cap[H_0^1(\Omega)]^3$ and $Q_{h,0} := Q_h\cap L_0^2(\Omega)$.
Combining the arguments in [12], [13] and [19], it is possible to show that the virtual space $\mathbf{V}_h$ has an optimal interpolation operator (see Lemma 5.2) and that the pair $(\mathbf{V}_h,Q_h)$ is inf-sup stable with $\beta_h>0$.
We have the following existence and convergence theorem that extends the analogous result for the two-dimensional case ([12]).

THEOREM 3.4. *Under the Assumptions* $(\mathbf{A1})-(\mathbf{A3})$, *let* $(\mathbf{u},p)\in[H_0^1(\Omega)]\times L_0^2(\Omega)$ *be the solution of the problem (2.1) and* $(\mathbf{u}_h,p_h)\in\mathbf{V}_{h,0}\times Q_{h,0}$ *be the unique solution of the problem (3.17). Assuming moreover* $\mathbf{u},\mathbf{f}\in[H^{s+1}(\Omega)]^3$ *and* $p\in H^s(\Omega)$, $0<s\le k$, *then:*

$$\begin{aligned} &|\mathbf{u}-\mathbf{u}_h|_1 \lesssim h^s\mathcal{F}(\mathbf{u},\nu) + h^{s+2}\mathcal{H}(\mathbf{f},\nu),\\ &\|p-p_h\|_0 \lesssim h^s|p|_s + h^s\mathcal{K}(\mathbf{u},\nu) + h^{s+2}|\mathbf{f}|_{s+1}, \end{aligned} \tag{3.18}$$

for suitable functions $\mathcal{F},\mathcal{H},\mathcal{K}$ *independent of* h.

Remark 3.5. Since the error of the velocity in (3.18) does not depend on the pressure, one can design a reduced scheme with a smaller number of dofs as for the two-dimensional case (Section 5.3 in [11]).

The discrete variational problem can be written as:

$$\begin{bmatrix} A & B^T \\ B & 0 \end{bmatrix} \begin{bmatrix} \mathbf{u} \\ p \end{bmatrix} = \begin{bmatrix} \mathbf{f} \\ 0 \end{bmatrix}, \tag{3.19}$$

where the matrices A and B are associated with the discrete bilinear forms $a_h(\cdot,\cdot)$ and $b_h(\cdot,\cdot)$. In the remainder of the paper, we omit the underscore h since we will always refer to the finite-dimensional space. We also write $\widehat{\mathbf{V}} \times Q$ instead of $\widehat{\mathbf{V}}_{h,0} \times Q_{h,0}$, only for the sake of simplifying the notation.

4. BDDC preconditioner. BDDC preconditioners [26] belong to the class of non-overlapping domain decomposition methods and they can be regarded as an evolution of Balancing Neumann Neumann preconditioners [27, 34]. They have been extensively applied to solve linear systems that arise from finite element discretizations of PDEs (see e.g. [31, 32, 33, 37]), and recently they have also been extended to VEM discretizations [14, 15, 17, 29, 30]. Here, we apply them to solve the saddle point linear system arising from the previous VEM discretization of three-dimensional Stokes equations. We first briefly resume the procedure to decompose the space of functions and to construct the preconditioner. The interested reader can obtain further details in [17].

4.1. Domain decomposition and saddle point problem. We decompose $\mathcal{T}_h$ into N non-overlapping subdomains Ω_i with characteristic size H_i:

$$\bar{\mathcal{T}}_h = \bigcup_{i=1}^{N} \bar{\Omega}_i, \qquad \Gamma = \bigcup_{i \neq j} \partial\Omega_i \cap \partial\Omega_j, \tag{4.1}$$

where each Ω_i is union of different polyhedra of the tassellation $\mathcal{T}_h$ and Γ is the interface (skeleton) among the subdomains.
We assume that the decomposition is shape-regular in the sense of [15]:
There exist a constant $\gamma^\star > 0$ and $N^\star > 0$ such that the subdomain decomposition satisfies the following properties:

- it is geometrically conforming, that is, for all i, if a vertex, edge, or face of Ω_i is contained in $\partial\Omega_i \cap \partial\Omega_j$, it is also, respectively, a vertex, edge, or face of Ω_j ;
- the subdomains Ω_i are shape regular of diameter H_i with constants $\gamma_{\Omega_i} > \gamma^\star$ and $N_{K,\Omega_i} < N_\star$;
- the decomposition is quasi-uniform: there exists an H such that for all i we have $H_i \simeq H$.

We will refer to the edges and faces of the subdomains Ω_i as macro edges and macro faces. We let $\mathcal{E}_H$, and $\mathcal{F}_H$ denote, respectively, the set of macro edges E and of macro faces F of the subdomain decomposition interior to Ω, and $\mathcal{F}_H^i$ and $\mathcal{E}_H^i$ denote the set of, respectively, macro faces and macro edges of the subdomain Ω^i.

We split the velocity components' dofs into boundary and interior parts. In particular, all the dofs $\mathbf{D}_V^4$ and $\mathbf{D}_V^5$ are classified as interior dofs, while the $\mathbf{D}_V^1$, $\mathbf{D}_V^2$ and $\mathbf{D}_V^3$ are split into dofs that belongs to a single subdomain Ω_i (internal) or that

belong to more than a single subdomain (boundary). We decompose the discrete velocity and pressure space $\widehat{\mathbf{V}}$ and Q into:

$$\widehat{\mathbf{V}} = \mathbf{V}_I \bigoplus \widehat{\mathbf{V}}_\Gamma, \quad Q = Q_I \bigoplus Q_0, \tag{4.2}$$

with $Q_0 := \prod_{i=1}^{N} \{q \in \Omega_i | q \textit{ is constant in } \Omega_i\}$. $\widehat{\mathbf{V}}_\Gamma$ is the continuous space of the traces on Γ of functions in $\widehat{\mathbf{V}}$, $\mathbf{V}_I$ and Q_I are direct sums of subdomain interior velocity spaces $\mathbf{V}_I^{(i)}$, and subdomain interior pressure spaces. We also define the space of interface velocity variables of the subdomain Ω_i by $\mathbf{V}_\Gamma^{(i)}$, and the associated product space by $\mathbf{V}_\Gamma = \prod_{i=1}^{N} \mathbf{V}_\Gamma^{(i)}$ of discontinuous functions across the interface.
The global saddle-point problem (3.19) can then be written as: find $(\mathbf{u}_I, p_I, \mathbf{u}_\Gamma, p_0) \in (\mathbf{V}_I, Q_I, \widehat{\mathbf{V}}_\Gamma, Q_0)$, such that:

$$\begin{bmatrix} A_{II} & B_{II}^T & \widehat{A}_{\Gamma I}^T & 0 \\ B_{II} & 0 & \widehat{B}_{I\Gamma} & 0 \\ \widehat{A}_{\Gamma I} & \widehat{B}_{I\Gamma}^T & \widehat{A}_{\Gamma\Gamma} & \widehat{B}_{0\Gamma}^T \\ 0 & 0 & \widehat{B}_{0\Gamma}^T & 0 \end{bmatrix} \begin{bmatrix} \mathbf{u}_I \\ p_I \\ \mathbf{u}_\Gamma \\ p_0 \end{bmatrix} = \begin{bmatrix} \mathbf{f}_I \\ 0 \\ \mathbf{f}_\Gamma \\ 0 \end{bmatrix}. \tag{4.3}$$

The blocks related to the continuous interface velocity are assembled from the corresponding subdomain submatrices, and the right-hand side vector $\mathbf{f}_I$ consists of subdomain vectors $\mathbf{f}_I^{(i)}$, and $\mathbf{f}_\Gamma$ is assembled from the subdomain components $\mathbf{f}_\Gamma^{(i)}$; we denote the spaces of the right-hand side vectors $\mathbf{f}_I$ and $\mathbf{f}_\Gamma$ by $\mathbf{F}_I$ and $\mathbf{F}_\Gamma$ respectively.

We proceed to eliminate, by static condensation, the independent subdomain variables $(\mathbf{u}_I, p_I)$ solving independent Dirichlet problems:

$$\begin{bmatrix} A_{II} & B_{II}^T \\ B_{II} & 0 \end{bmatrix} \begin{bmatrix} \mathbf{u}_I \\ p_I \end{bmatrix} + \begin{bmatrix} \widehat{A}_{\Gamma I}^T & 0 \\ \widehat{B}_{I\Gamma} & 0 \end{bmatrix} \begin{bmatrix} \mathbf{u}_\Gamma \\ p_0 \end{bmatrix} = \begin{bmatrix} \mathbf{f}_I \\ 0 \end{bmatrix}, \tag{4.4}$$

and obtain the global interface saddle point problem:

$$\widehat{S}\,\widehat{u} = \begin{bmatrix} \widehat{S}_\Gamma & \widehat{B}_{0\Gamma}^T \\ \widehat{B}_{0\Gamma} & 0 \end{bmatrix} \begin{bmatrix} \mathbf{u}_\Gamma \\ p_0 \end{bmatrix} = \begin{bmatrix} \mathbf{g}_\Gamma \\ 0 \end{bmatrix} = \widehat{\mathbf{g}}, \tag{4.5}$$

where the right-hand side $\widehat{\mathbf{g}} \in \mathbf{F}_\Gamma \times F_0$ is given by

$$\widehat{\mathbf{g}} = \sum_{i=1}^{N} {R_\Gamma^{(i)}}^T \left\{ \begin{bmatrix} \mathbf{f}_\Gamma^{(i)} \\ 0 \end{bmatrix} - \begin{bmatrix} A_{\Gamma I}^{(i)} & {B_{I\Gamma}^{(i)}}^T \\ 0 & 0 \end{bmatrix} \begin{bmatrix} A_{II}^{(i)} & {B_{II}^{(i)}}^T \\ B_{II}^{(i)} & 0 \end{bmatrix}^{-1} \begin{bmatrix} \mathbf{f}_I^{(i)} \\ 0 \end{bmatrix} \right\}. \tag{4.6}$$

$R_\Gamma^{(i)} : \widehat{\mathbf{V}}_\Gamma \to \mathbf{V}_\Gamma^{(i)}$ is the operator which maps functions in the continuous interface velocity space $\widehat{\mathbf{V}}_\Gamma$ to their subdomain components in the space $\mathbf{V}_\Gamma^{(i)}$. We denote the direct sum of the $R_\Gamma^{(i)}$ with R_Γ.
$\widehat{S}_\Gamma$ is assembled from the subdomain Stokes Schur complements $S_\Gamma^{(i)}$, which are defined by: given $\mathbf{w}_\Gamma^{(i)} \in \mathbf{V}_\Gamma^{(i)}$, determine $S_\Gamma^{(i)} \mathbf{w}_\Gamma^{(i)} \in \mathbf{F}_\Gamma^{(i)}$ such that

$$\begin{bmatrix} A_{II}^{(i)} & {B_{II}^{(i)}}^T & {A_{\Gamma I}^{(i)}}^T \\ B_{II}^{(i)} & 0 & B_{I\Gamma}^{(i)} \\ A_{\Gamma I}^{(i)} & {B_{I\Gamma}^{(i)}}^T & A_{\Gamma\Gamma}^{(i)} \end{bmatrix} \begin{bmatrix} \mathbf{w}_I^{(i)} \\ q_I^{(i)} \\ \mathbf{w}_\Gamma^{(i)} \end{bmatrix} = \begin{bmatrix} \mathbf{0} \\ 0 \\ S_\Gamma^{(i)} \mathbf{w}_\Gamma^{(i)} \end{bmatrix}, \tag{4.7}$$

these Schur complements are symmetric and positive definite (Lemma 5.1 in [17]). Denoting by S_Γ the direct sum of the $S_\Gamma^{(i)}$, then $\widehat{S}_\Gamma$ is given by

$$\widehat{S}_\Gamma = R_\Gamma^T S_\Gamma R_\Gamma = \sum_{i=1}^{N} {R_\Gamma^{(i)}}^T S_\Gamma^{(i)} R_\Gamma^{(i)}. \tag{4.8}$$

Remark 4.1. The BDDC preconditioner that we will introduce in the next Section for problem (4.5), makes the operator of the preconditioned problem symmetric and positive definite on the so-called "benign space", so we will be able to use the preconditioned conjugate gradient (CG) method to accelerate the solution.

4.2. Construction of the preconditioner and convergence rate. Following the standard BDDC framework for FEM [33], we mainly need to introduce two ingredients to handle this type of algorithm:

- $\widetilde{\mathbf{V}}_\Gamma = \widehat{\mathbf{V}}_\Pi \bigoplus \mathbf{V}_\Delta = \widehat{\mathbf{V}}_\Pi \bigoplus \left(\prod_{i=1}^{N} \mathbf{V}_\Delta^{(i)}\right)$, that it is a partially assembled interface velocity space where, $\widehat{\mathbf{V}}_\Pi$ is the continuous coarse-level primal velocity space and $\mathbf{V}_\Delta$ is the complementary discontinuous one;
- an average operator $E_D = \widetilde{R}\widetilde{R}_D^T$, which maps $\widetilde{\mathbf{V}}_\Gamma \times Q_0$, with generally discontinuous interface velocities, to elements with continuous interface velocities in the same space. Here, $\widetilde{R}$ is defined by simply extending the interface restriction operator $\widetilde{R}_\Gamma : \widehat{\mathbf{V}}_\Gamma \to \widetilde{\mathbf{V}}_\Gamma$ to the space of piecewise constant pressures. $\widetilde{R}_{D,\Gamma}$ is its scaled version for which it holds $\widetilde{R}^T \widetilde{R}_{D,\Gamma} = I$.

The preconditioner for solving the global saddle-point problem (4.5) is then:

$$M^{-1} = \widetilde{R}_D^T \widetilde{S}^{-1} \widetilde{R}_D, \tag{4.9}$$

where $\widetilde{S}$ is the Schur complement system that arises using the partially assembled velocity interface functions. The action of this preconditioner can be split as a sum of a coarse saddle point problem defined on the interface and local problems on each subdomain.

Remark 4.2. As in the VEM two-dimensional case and in the FEM framework, the preconditioned problem is symmetric and positive definite on the so-called "benign space" $\widehat{\mathbf{V}}_{\Gamma,B} \times Q_0$ and $\widetilde{\mathbf{V}}_{\Gamma,B} \times Q_0$, where:

$$\widehat{\mathbf{V}}_{\Gamma,B} = \{\mathbf{v}_\Gamma \in \widehat{\mathbf{V}}_\Gamma | \widehat{B}_{0\Gamma} \mathbf{v}_\Gamma = 0\} \quad \text{and} \quad \widetilde{\mathbf{V}}_{\Gamma,B} = \{\mathbf{v}_\Gamma \in \widetilde{\mathbf{V}}_\Gamma | \widetilde{B}_{0\Gamma} \mathbf{v}_\Gamma = 0\}.$$

This is a crucial observation, and, to ensure that the iterates of the preconditioned iterative method remain in this subspace, it is necessary that a no-net-flux condition (Assumption 1) holds:

ASSUMPTION 1. *For any* $\mathbf{v}_\Delta \in \mathbf{V}_\Delta$, $\int_{\partial\Omega_i} \mathbf{v}_\Delta^{(i)} \cdot \mathbf{n} = 0$ *and* $\int_{\partial\Omega_i} (E_D \mathbf{v}_\Delta)^{(i)} \cdot \mathbf{n} = 0$, *where* $\mathbf{n}$ *is the outward normal of* $\partial\Omega_i$. *We can equivalently write* $B_{0\Delta}^{(i)} \mathbf{v}_\Delta^{(i)} = 0$ *and* $B_{0\Delta}^{(i)} (E_D \mathbf{v}_\Delta)^{(i)} = 0$.

The convergence rate of the preconditioned conjugate gradient method with a BDDC preconditioner is instead characterized by the stability of the norm of the average operator E_D:

ASSUMPTION 2. *There exists a positive constant* C, *which is independent of* H, h, *and the number of subdomains, such that*

$$|\bar{R}_\Gamma (E_{D,\Gamma} \mathbf{v}_\Gamma)|_{E(\Gamma)} \leq C \left(1 + \log\left(\frac{H}{h}\right)\right) |\bar{R}_\Gamma \mathbf{v}_\Gamma|_{E(\Gamma)}, \quad \forall \mathbf{v}_\Gamma \in \widetilde{\mathbf{V}}_\Gamma.$$

where $\bar{R}_\Gamma : \widetilde{\mathbf{V}}_\Gamma \to \mathbf{V}_\Gamma$ maps a velocity function from the partially assembled space into the product one and we equipped the space $\mathbf{V}_\Gamma^{(i)}$ with the seminorm introduced in Lemma 2.2, and consequently the space $\mathbf{V}_\Gamma$ with the seminorm $|\mathbf{v}_\Gamma|^2_{E(\Gamma)} = \sum_{i=1}^N \mathbf{v}_\Gamma^{(i)}|^2_{E(\Gamma_i)}$.
Assumptions 1 and 2 are satisfied only for suitable choices of the primal dofs as we wil show in Section 5. Combining them we have the quasi-optimal estimate [17]:

THEOREM 4.3. *Let Assumptions 1 and 2 hold. Then, the preconditioned operator $M^{-1}\widehat{S}$ is symmetric positive definite with respect to the bilinear form $\langle\cdot,\cdot\rangle_{\widehat{S}}$ on the benign space $\widehat{\mathbf{V}}_{\Gamma,B} \times Q_0$. Its minimum eigenvalue is 1 and its maximum eigenvalue is bounded by*

$$C\frac{1}{\beta_h^2}\left(1+\log\left(\frac{H}{h}\right)\right)^2. \tag{4.10}$$

Here, C is a constant independent of H, h, and the number of subdomains, and β_h is the discrete inf-sup stability constant.

5. Some auxiliary Lemmas. In this section, we define some seminorms and we recall some auxiliary lemmas that we need in the following section to satisfy the Assumption 1 and 2.
Firstly, we introduce the $|.|_{S_\Gamma^{(i)}}$ and $|.|_{S_\Gamma}$ seminorms defined by

$$|\mathbf{v}_\Gamma^{(i)}|^2_{S_\Gamma^{(i)}} = {\mathbf{v}_\Gamma^{(i)}}^T S_\Gamma^{(i)} \mathbf{v}_\Gamma^{(i)}, \quad |\mathbf{v}_\Gamma|^2_{S_\Gamma} = {\mathbf{v}_\Gamma}^T S_\Gamma \mathbf{v}_\Gamma = \sum_{i=1}^N |\mathbf{v}_\Gamma^{(i)}|^2_{S_\Gamma^{(i)}}, \tag{5.1}$$

and a seminorm on the space $\widetilde{\mathbf{V}}_\Gamma$:

$$|\mathbf{v}_\Gamma|^2_{\widetilde{S}_\Gamma} = \mathbf{v}_\Gamma^T \bar{R}_\Gamma^T S_\Gamma \bar{R}_\Gamma \mathbf{v}_\Gamma = |\mathbf{v}_\Gamma|^2_{S_\Gamma}, \qquad \forall \mathbf{v}_\Gamma \in \widetilde{\mathbf{V}}_\Gamma.$$

We recall Lemma 5.2 in [17], that gives us the equivalence of the seminorm just introduced and the one defined in Lemma 2.2:

LEMMA 5.1. *There exist positive constant c_1 and c_2, independent of H, h and the shape of subdomains, such that*

$$c_1 {\beta_h}^2 |\mathbf{v}_\Gamma|^2_{S_\Gamma} \le |\mathbf{v}_\Gamma|^2_{E(\Gamma)} \le c_2 |\mathbf{v}_\Gamma|^2_{S_\Gamma} \quad \forall \mathbf{v}_\Gamma \in \mathbf{V}_\Gamma,$$

where β_h is the discrete inf-sup stability constant.

We need an optimal VEM interpolant designed for a Stokes problem (for the proof see the technical report of the present paper published in [16]) and a Riesz Basis Property, that gives us the equivalence between the $L^2(f)$ norm of a function in $\widehat{\mathbb{B}}_k(f)$ and the euclidean norm of the vector of its dofs, see Lemma 5.2 and 5.3, respectively.

LEMMA 5.2. *Let $\mathbf{v} \in [H^{1+s}(K)]^3$, $0 \le s \le 1$, there exist $\mathbf{v}_I \in \mathbf{V}_h(K)$ s.t.:*

$$\|\mathbf{v} - \mathbf{v}_I\|_{0,K} + |\mathbf{v} - \mathbf{v}_I|_{1,K} \le h^{1+s} |\mathbf{v}|_{1+s,\widetilde{K}}.$$

LEMMA 5.3. *Let be f a face of an element K. For all $\mathbf{v}_h \in [\widehat{\mathbb{B}}_k(f)]^3$ we have:*

$$\int_f |\mathbf{v}_h|^2 \simeq h^2 \sum_{i \in \mathcal{X}} |\mathbf{D}^i_{\mathbf{v}}(\mathbf{v}_h)|^2, \tag{5.2}$$

where $\mathcal{X}$ is the union of the set of dofs $\mathbf{D}^1_{\mathbf{v}}, \mathbf{D}^2_{\mathbf{v}}$ and $\mathbf{D}^3_{\mathbf{v}}$.

We do not provide the proof of this second Lemma because it is the natural vector extension of the ones in [15] and [22], with a slightly different choice for the dofs of the face velocity space. Moreover, it simply involves the Π^0_{k+1} projection instead of Π^0_k.

Finally we need to recall two lemmas that we need for estimating the contributions of the interface velocity functions defined on the edges and faces of the subdomains. The first one is the vectorial extension of the one in [15], and the second is a *face lemma*, see Lemma 5.4 and 5.5.

LEMMA 5.4. *Let be Ω_i a subdomain and let be F a face of Ω_i. Then for $\mathbf{v}_\Gamma \in \mathbf{V}_{\Gamma|F}$ we have*

$$\|\mathbf{v}_\Gamma\|_{[L^2(\partial F)]^3} \lesssim \sqrt{1+\log(H/h)}\|\mathbf{v}_\Gamma\|_{[H^{1/2}(F)]^3}, \tag{5.3}$$

where the subscript $|F$ means that we are restricting the interface space $\mathbf{V}_\Gamma$ on the face F.

LEMMA 5.5. *Let $\mathbf{v}_\Gamma \in \mathbf{V}^{(i)}_\Gamma$. Then, for all faces F of Ω_i it holds that $\theta_{\mathcal{F}_i}\mathbf{v}_{\Gamma|F} \in [H^{1/2}_{00}(F)]^3$ and*

$$\|\theta_{\mathcal{F}_i}\mathbf{v}_\Gamma\|^2_{[H^{1/2}_{00}(F)]^3} \lesssim (1+\log(H/h))^2\|\mathbf{v}_\Gamma\|^2_{[H^{1/2}(F)]^3}, \tag{5.4}$$

where $[H^{1/2}_{00}(F)]^3$ is the space of functions $\mathbf{v}$ whose extention by zero $\widehat{\mathbf{v}} \in [H^{1/2}(\mathbb{R})^2]^3$ and it is equipped with the norm $\|\mathbf{v}\|_{[H^{1/2}_{00}(F)]^3} = \|\widehat{\mathbf{v}}\|_{[H^{1/2}(\mathbb{R}^2)]^3}$.

The proof of this lemma follows the same procedure of the one in [15], where we use Lemma 5.2 to substitute the Scott-Zangh interpolation and Lemma 5.3 adapted in our framework.

6. No-net flux condition and stability of the average operator. In this section we provide a recipe to construct the coarse space in three dimensions. Following [33], we recall that in three dimensions, the interface Γ of a subdomain Ω_i is constituted by faces $\mathcal{F}_l$ shared by two subdomains, edges $\mathcal{E}_k$ that are shared by more than two subdomains (the notation $\mathcal{E}_k(\mathcal{F}_l)$ is to underline that the edge $\mathcal{E}_k$ belongs to the boundary of face $\mathcal{F}_l$) and vertices V_j that are the endpoints of the edges. Now let be G any one of these geometrical entities and let be $\mathbf{v} \in \mathbf{V}$ a generic virtual function, we define the cut-off linear functional θ_G that maps a virtual function $\mathbf{v}$ into another virtual function $\theta_G(\mathbf{v})$, that is equal to $\mathbf{v}$ on all the dofs that belongs to G and 0 elsewhere, for simplicity we generally write $\theta_G\mathbf{v}$ instead of $\theta_G(\mathbf{v})$. We use the subscript $\mathcal{F}_l$ to refer the dofs that live only in the interior of the face excluding the boundary face dofs. When a multi-subscript is present, like $\mathcal{F}_{ij}$, it means that the face is shared between the subdomains Ω_i and Ω_j.

Our proof will be for the standard cardinality scaling, where $\widetilde{R}_D$ is obtained by multiplying each row of $\widetilde{R}$ that corresponds to a dual dof by $\delta^\dagger(x) := 1/card(I_x), \forall x \in \Gamma$, where I_x is the set of subdomains' indices that have the node x on their boundaries, and $card(\cdot)$ denotes the cardinality of the set. It is easy to extend it to a general scaling using the same techniques as in [37].

To satisfy Assumption 1, we first make all vertices primal, and then we require that, for any $\mathbf{v}_\Delta$, the two quantities:

$$\int_{\mathcal{F}_{ij}} \mathbf{v}^{(i)}_\Delta \cdot \mathbf{n}_{ij} = \int_{\mathcal{F}_{ij}} (\theta_{\mathcal{F}_{ij}}\mathbf{v}^{(i)}_\Delta)\cdot\mathbf{n}_{ij} + \sum_{\mathcal{E}_k \subset \mathcal{F}_{ij}} \int_{\mathcal{F}_{ij}} (\theta_{\mathcal{E}_k(\mathcal{F}_{ij})}\mathbf{v}^{(i)}_\Delta)\cdot\mathbf{n}_{ij} \tag{6.1}$$

and

$$\int_{\mathcal{F}_{ij}} (E_D \mathbf{v})^{(i)}_{\Delta} \cdot \mathbf{n}_{ij} = \frac{1}{2} \int_{\mathcal{F}_{ij}} \theta_{\mathcal{F}_{ij}} (\mathbf{v}^{(i)}_{\Delta} + \mathbf{v}^{(j)}_{\Delta}) \cdot \mathbf{n}_{ij} + \sum_{\mathcal{E}_k \subset \mathcal{F}_{ij}} \sum_{m \in \mathcal{N}_{\mathcal{E}_k}} \frac{1}{card(\mathcal{N}_{\mathcal{E}_k})} \int_{\mathcal{F}_{ij}} (\theta_{\mathcal{E}_k(\mathcal{F}_{ij})} \mathbf{v}^{(m)}_{\Delta}) \cdot \mathbf{n}_{ij} \tag{6.2}$$

vanish, where $\mathcal{N}_{\mathcal{E}_k}$ is the set of all the subdomains that share the edge $\mathcal{E}_k$ and $\mathbf{n}_{ij}$ is the unit outward normal vector to the face $\mathcal{F}_{ij}$. To do so, we need that all the integrals of the right-hand side of (6.1) and (6.2) will vanish. This can be achieved by enforcing a primal constraint for each face $\mathcal{F}_{ij}$:

$$\int_{\mathcal{F}_{ij}} (\theta_{\mathcal{F}_{ij}} \mathbf{v}^{(i)}_{\Gamma}) \cdot \mathbf{n}_{ij} = \int_{\mathcal{F}_{ij}} (\theta_{\mathcal{F}_{ij}} \mathbf{v}^{(j)}_{\Gamma}) \cdot \mathbf{n}_{ij} \tag{6.3}$$

and a set of primal constraints requiring that for each edge $\mathcal{E}_k$, on each face $\mathcal{F}_{ij}$, the following quantity is the same for all $m \in \mathcal{N}_{\mathcal{E}_k}$:

$$\int_{\mathcal{F}_{ij}} (\theta_{\mathcal{E}_k(\mathcal{F}_{ij})} \mathbf{v}^{(m)}_{\Gamma}) \cdot \mathbf{n}_{ij} \tag{6.4}$$

To ensure constraint (6.3), we need one primal variable per face, while, to ensure constraint (6.4), we need as many primal variables as the number of faces which share the edge $\mathcal{E}_k$. We remark that in our VEM context, the quantities in (6.3) and (6.4) are directly computable from the dofs introduced in Section 3. For particular subdomain partitions, such as those with cubic subdomains and hexahedral elements, it might happen that some of the primal basis functions are linearly dependent; this situation is harmless in practice since we can perform a singular value decomposition of the basis dofs and obtain non-singular coarse operators.

To satisfy Assumption 2, we have to ensure that we have the right type of constraints that can control the rigid body modes (at least six constraints: the three translations and the three rotations). Given the fact that the coefficients of the Stokes problem are all the same for each subdomain and that the vertices of the subdomains have been selected as primal constraints, we can prove that the second Assumption is satisfied if also all the faces of the interface Γ are *fully primal* in the sense of the following definition (see [31, def. 5.3]):

DEFINITION 6.1. *A face $\mathcal{F}_{ij}$ is called fully primal if, in the space of primal constraints over $\mathcal{F}_{ij}$, there exists a set f_m, $m = 1, ..., 6$, of linear functionals on $\mathbf{V}^{(i)}_{\Gamma}$ with the following properties:*

- $|f_m(\mathbf{v}^{(i)}_{\Gamma})|^2 \leq CH^{-1}(1 + \log(H/h)) \|\mathbf{v}^{(i)}_{\Gamma}\|_{H^{1/2}(\mathcal{F}_{ij})}$;
- $f_m(\mathbf{r}_l) = \delta_{ml} \quad \forall m, l = 1, ..., 6 \quad \mathbf{r}_l \in ker(\varepsilon)$,

with $C > 0$ and $\mathbf{v}^{(i)}_{\Gamma} \in \mathbf{V}^{(i)}_{\Gamma}$.

We recall that, to satisfy Assumption 1, we have chosen as primal constraints some averages of the normal component of the velocity over the edges. In Section 7 of [33] (see also further details in [31]), it is shown that this choice of primal dofs is sufficient to guarantee a set of functionals that makes the face fully primal. It is essential to underline that in some particular cases, like triangular or rectangular faces, some of these constraints can be linearly dependent and it is necessary to introduce some extra edge average in the tangential direction. This condition can

be verified numerically because the selection of a set of linearly independent set of constraints can be computed using a QR factorization and selecting six functionals that are robustly independent.
We are ready to state the lemma related to the stability of the average operator:

LEMMA 6.2. *For all* $\mathbf{v}_\Gamma \in \widetilde{\mathbf{V}}_\Gamma$ *holds that:*

$$|E_D\mathbf{v}_\Gamma|^2_{\widetilde{S}} \lesssim C\frac{1}{\beta^2}\left(1+\log\left(\frac{H}{h}\right)\right)^2 |\mathbf{v}_\Gamma|^2_{\widetilde{S}}, \tag{6.5}$$

where C *is a positive constant that is independent on* h, H *and* β_h*, but it can depend on the degree* k *of the virtual element discretization.*

Proof. Let consider $\mathbf{v}_\Gamma \in \widetilde{\mathbf{V}}_\Gamma$ and we define $\mathbf{w}_\Gamma := E_D\mathbf{v}_\Gamma$. We have:

$$|\mathbf{w}_\Gamma|_{\widetilde{S}} = |\mathbf{w}_\Gamma - \mathbf{v}_\Gamma + \mathbf{v}_\Gamma|_{\widetilde{S}} \leq |\mathbf{w}_\Gamma - \mathbf{v}_\Gamma|_{\widetilde{S}} + |\mathbf{v}_\Gamma|_{\widetilde{S}}. \tag{6.6}$$

Since all the vertices of the subdomains are primal, we can rewrite:

$$|\mathbf{w}_\Gamma - \mathbf{v}_\Gamma|_{\widetilde{S}_\Gamma} = \sum_{i=1}^{N} |\mathbf{w}_\Gamma^{(i)} - \mathbf{v}_\Gamma^{(i)}|_{S_\Gamma^{(i)}} \tag{6.7}$$

and for each subdomain Ω_i we can also use the split:

$$\mathbf{w}_\Gamma^{(i)} - \mathbf{v}_\Gamma^{(i)} = \sum_{\mathcal{F}_{ij}\subset\partial\Omega_i} \theta_{\mathcal{F}_{ij}}(\mathbf{w}_\Gamma^{(i)} - \mathbf{v}_\Gamma^{(i)}) + \sum_{\mathcal{E}_k\subset\partial\Omega_i} \theta_{\mathcal{E}_k}(\mathbf{w}_\Gamma^{(i)} - \mathbf{v}_\Gamma^{(i)}) \tag{6.8}$$

Recalling that a face $\mathcal{F}_{ij}$ is shared by two subdomains i, j and using the explicit definition of E_D:

$$\mathbf{w}_\Gamma^{(i)} - \mathbf{v}_\Gamma^{(i)} = \frac{1}{2}(\mathbf{v}_\Gamma^{(i)} + \mathbf{v}_\Gamma^{(j)}) - \mathbf{v}_\Gamma^{(i)} = \mathbf{v}_\Gamma^{(j)} - \mathbf{v}_\Gamma^{(i)}.$$

Starting from the face contributions, we write:

$$\mathbf{v}_\Gamma^{(j)} - \mathbf{v}_\Gamma^{(i)} = \left(\mathbf{v}_\Gamma^{(j)} - \sum_{m=1}^{6} f_m^{\mathcal{F}_{ij}}(\mathbf{v}_\Gamma^{(j)})\mathbf{r}_m\right) - \left(\mathbf{v}_\Gamma^{(i)} - \sum_{m=1}^{6} f_m^{\mathcal{F}_{ij}}(\mathbf{v}_\Gamma^{(i)})\mathbf{r}_m\right) \tag{6.9}$$

where $\{\mathbf{r}_m\}$ for $m = 1, .., 6$ is the basis for the rigid body modes and the $f_m^{\mathcal{F}_{ij}}(\cdot)$ are the functionals that are equal for the faces i and j since the faces are fully primal. For an arbitrary rigid body mode, $\mathbf{r}^{(i)} \in \mathbf{V}_\Gamma^{(i)}$ we write:

$$\mathbf{v}_\Gamma^{(i)} - \sum_{m=1}^{6} f_m^{\mathcal{F}_{ij}}(\mathbf{v}_\Gamma^{(i)})\mathbf{r}_m = (\mathbf{v}_\Gamma^{(i)} - \mathbf{r}^{(i)}) - \sum_{m=1}^{6} f_m^{\mathcal{F}_{ij}}(\mathbf{v}_\Gamma^{(i)} - \mathbf{r}^{(i)})\mathbf{r}_m \tag{6.10}$$

We can estimate the first term of the right-hand side using lemma 5.5:

$$\|\theta_{\mathcal{F}_{ij}}(\mathbf{v}_\Gamma^{(i)} - \mathbf{r}^{(i)})\|_{[H^{1/2}_{00}(\mathcal{F}_{ij})]^3} \lesssim (1+\log(H/h))\|\mathbf{v}_\Gamma^{(i)} - \mathbf{r}^{(i)}\|_{[H^{1/2}(\mathcal{F}_{ij})]^3}. \tag{6.11}$$

Then we consider the second term of (6.10), and we estimate it using two additional contributions, by lemma 8 in [31]:

$$\|\theta_{\mathcal{F}_{ij}}\mathbf{r}_m^{(i)}\|_{[H^{1/2}_{00}(\mathcal{F}_{ij})]^3} \lesssim H(1+\log(H/h)) \tag{6.12}$$

and by the definition of fully primal face (6.1) and (5.4) we have:

$$|f_m^{\mathcal{F}_{ij}}(\mathbf{v}_\Gamma^{(i)} - \mathbf{r}^{(i)})| \lesssim \frac{1}{H}(1+\log(H/h))\|\mathbf{v}_\Gamma^{(i)} - \mathbf{r}^{(i)}\|_{[H^{1/2}(\mathcal{F}_{ij})]^3}. \tag{6.13}$$

Then combining the previous two estimates we have:

$$\|\theta_{\mathcal{F}_{ij}} \sum_{m=1}^{6} f_m^{\mathcal{F}_{ij}}(\mathbf{v}_\Gamma^{(i)} - \mathbf{r}^{(i)})\mathbf{r}_m\|_{[H_{00}^{1/2}(\mathcal{F}_{ij})]^3} \lesssim (1+\log(H/h))\|\mathbf{v}_\Gamma^{(i)} - \mathbf{r}^{(i)}\|_{[H^{1/2}(\mathcal{F}_{ij})]^3}. \tag{6.14}$$

By triangular inequality and since $\mathbf{r}^{(i)}$ is an arbitrary rigid body mode, we can take the minimum of over all the modes and by Lemma 2.2:

$$\begin{aligned}\|\theta_{\mathcal{F}_{ij}}(\mathbf{v}_\Gamma^{(i)} - \sum_{m=1}^{6} f_m^{\mathcal{F}_{ij}}(\mathbf{v}_\Gamma^{(i)})\mathbf{r}_m)\|_{[H_{00}^{1/2}(\mathcal{F}_{ij})]^3} &\lesssim \|\theta_{\mathcal{F}_{ij}}(\mathbf{v}_\Gamma^{(i)} - \mathbf{r}^{(i)})\|_{[H_{00}^{1/2}(\mathcal{F}_{ij})]^3} + \\ \|\theta_{\mathcal{F}_{ij}}(\mathbf{v}_\Gamma^{(i)} - \sum_{m=1}^{6} f_m^{\mathcal{F}_{ij}}(\mathbf{v}_\Gamma^{(i)} - \mathbf{r}^{(i)})\mathbf{r}_m)\|_{[H_{00}^{1/2}(\mathcal{F}_{ij})]^3} &\lesssim \\ (1+\log(H/h))\|\mathbf{v}_\Gamma^{(i)} - \mathbf{r}^{(i)}\|_{[H^{1/2}(\mathcal{F}_{ij})]^3} &\lesssim (1+\log(H/h))|\mathbf{v}_\Gamma^{(i)}|_{[H^{1/2}(\mathcal{F}_{ij})]^3}\end{aligned} \tag{6.15}$$

We can repeat in the same way for the jth term and obtain:

$$\begin{aligned}\|\theta_{\mathcal{F}_{ij}}(\mathbf{v}_\Gamma^{(i)} - \mathbf{v}_\Gamma^{(j)})\|_{[H_{00}^{1/2}(\mathcal{F}_{ij})]^3} &\lesssim (1+\log(H/h))|\mathbf{v}_\Gamma^{(i)}|_{[H^{1/2}(\mathcal{F}_{ij})]^3} \\ &+(1+\log(H/h))|\mathbf{v}_\Gamma^{(j)}|_{[H^{1/2}(\mathcal{F}_{ij})]^3}\end{aligned} \tag{6.16}$$

Regarding the edge terms, we need to estimate contributions that depend on the number of subdomains that share the edge. We propose the estimate for one of these contributions since the others are treated similarly. We consider an edge $\mathcal{E}_k \subset \partial\mathcal{F}_{ij}$, by the fact that all the faces are fully primal, we can reduce these terms to face estimates, we write:

$$\begin{aligned}\|\mathbf{v}_\Gamma^{(i)} - \mathbf{v}_\Gamma^{(j)}\|^2_{[L^2(\mathcal{E}_k)]^3} &\lesssim \|\mathbf{v}_\Gamma^{(i)} - \sum_{m=1}^{6} f_m^{\mathcal{F}_{ij}}(\mathbf{v}_\Gamma^{(i)})\mathbf{r}_m\|^2_{[L^2(\mathcal{E}_k)]^3} \\ &+\|\mathbf{v}_\Gamma^{(j)} - \sum_{m=1}^{6} f_m^{\mathcal{F}_{ij}}(\mathbf{v}_\Gamma^{(j)})\mathbf{r}_m\|^2_{[L^2(\mathcal{E}_k)]^3}\end{aligned} \tag{6.17}$$

We proceed again considering an arbitrary rigid body mode $\mathbf{r}^{(i)} \in \mathbf{V}_\Gamma^{(i)}$. Using the triangular inequality and (5.4):

$$\begin{aligned}\|\mathbf{v}_\Gamma^{(i)} - \sum_{m=1}^{6} f_m^{\mathcal{F}_{ij}}(\mathbf{v}_\Gamma^{(i)})\mathbf{r}_m\|^2_{[L^2(\mathcal{E}_k)]^3} &\lesssim \|\mathbf{v}_\Gamma^{(i)} - \mathbf{r}^{(i)}\|_{[L^2(\mathcal{E}_k)]^3} + \\ \|\sum_{m=1}^{6} f_m^{\mathcal{F}_{ij}}(\mathbf{v}_\Gamma^{(i)} - \mathbf{r}^{(i)})\mathbf{r}_m\|^2_{[L^2(\mathcal{E}_k)]^3} &\lesssim (1+\log(H/h))\|\mathbf{v}_\Gamma^{(i)}\|^2_{[H^{1/2}(\mathcal{F}_{ij})]^3} + \\ &\sum_{m=1}^{6} |f_m^{\mathcal{F}_{ij}}(\mathbf{v}_\Gamma^{(i)} - \mathbf{r}^{(i)})|^2\|\mathbf{r}_m\|^2_{[L^2(\mathcal{E}_k)]^3}.\end{aligned} \tag{6.18}$$

It can be proved that $\|\mathbf{r}_m\|_{[L^2(\mathcal{E}_k)]^3} \lesssim H$ ([32]), and now using (6.13) and minimizing again on all over the rigid body modes:

$$\|\mathbf{v}_\Gamma^{(i)} - \sum_{m=1}^{6} f_m^{\mathcal{F}_{ij}}(\mathbf{v}_\Gamma^{(i)})\mathbf{r}_m\|^2_{[L^2(\mathcal{E}_k)]^3} \lesssim (1+\log(H/h))|\mathbf{v}_\Gamma^{(j)}|^2_{[H^{1/2}(\mathcal{F}_{ij})]^3}. \tag{6.19}$$

We have an analogous result for the jth term and obtain:

$$\begin{aligned}\|\mathbf{v}_\Gamma^{(i)} - \mathbf{v}_\Gamma^{(j)}\|^2_{[L^2(\mathcal{E}_k)]^3} \lesssim (1+\log(H/h))|\mathbf{v}_\Gamma^{(i)}|^2_{[H^{1/2}(\mathcal{F}_{ij})]^3} \\ +(1+\log(H/h))|\mathbf{v}_\Gamma^{(j)}|^2_{[H^{1/2}(\mathcal{F}_{ij})]^3}.\end{aligned} \tag{6.20}$$

We conclude by Lemma 5.1, combining (6.16) and (6.20) by summing over the subdomains. ∎

Assumption 2 is then obtained by combining Lemma 6.2 and 5.1.

7. Adaptivity. We recall here an adaptive technique to enrich the minimal primal space $\mathbf{V}_\Gamma$ [25, 36]. The idea is to solve generalized eigenvalue problems defined on each subdomain face $\mathcal{F}$ and edge $\mathcal{E}$ and then construct an enriched primal space such that the condition number of the preconditioned system will be bounded from above by a selected $\nu_{tol} \in [1,\infty)$ times a constant independent on h, H and N. To construct an adaptive coarse space, we need to settle in a deluxe scaling context [37]. For each face $\mathcal{F}$ shared by two subdomains i, j, we consider the principal minors of the subdomain matrices $S_T^{(k)}$ with $k = i, j$:

$$S_{\mathcal{F}\mathcal{F}}^{(k)} := R_{\mathcal{F}}^{(k)} S_T^{(k)} {R_{\mathcal{F}}^{(k)}}^T, \tag{7.1}$$

where $R_{\mathcal{F}}^{(k)}$ maps $\mathbf{V}_\Gamma^{(k)}$ to the dofs located on F. Then we split the matrices as follows

$$S_{\mathcal{F}\mathcal{F}}^{(k)} = \begin{bmatrix} S_{\mathcal{F}'\mathcal{F}'}^{(k)} & S_{F'F_\Delta}^{(k)} \\ {S_{\mathcal{F}'\mathcal{F}_\Delta}^{(k)}}^T & S_{\mathcal{F}_\Delta\mathcal{F}_\Delta}^{(k)} \end{bmatrix}, \qquad k = i, j \tag{7.2}$$

where $\mathcal{F}_\Delta$ is the dual set of the dofs associated to the face $\mathcal{F}$ and $\mathcal{F}' := \Gamma_i \setminus \mathcal{F}_\Delta$. We introduce the Schur complements:

$$\widetilde{S}_{\mathcal{F}_\Delta\mathcal{F}_\Delta}^{(k)} = S_{\mathcal{F}_\Delta\mathcal{F}_\Delta}^{(k)} - {S_{\mathcal{F}'\mathcal{F}_\Delta}^{(k)}}^T {S_{\mathcal{F}'\mathcal{F}'}^{(k)}}^{-1} S_{\mathcal{F}'\mathcal{F}_\Delta}^{(k)}, \quad k = i, j. \tag{7.3}$$

and then we solve the following eigenvalue problems:

$$\widetilde{S}_{\mathcal{F}_\Delta\mathcal{F}_\Delta}^{(i)} : \widetilde{S}_{\mathcal{F}_\Delta\mathcal{F}_\Delta}^{(j)} \psi = \nu S_{\mathcal{F}_\Delta\mathcal{F}_\Delta}^{(i)} : S_{\mathcal{F}_\Delta\mathcal{F}_\Delta}^{(j)} \psi \tag{7.4}$$

where $A : B = (A^{-1} + B^{-1})^{-1}$, finally we choose the element of the primal space as $S_{\mathcal{F}_\Delta\mathcal{F}_\Delta}^{(i)} : S_{\mathcal{F}_\Delta\mathcal{F}_\Delta}^{(j)} \Psi$, where Ψ is the matrix formed column-wise by those eigenvectors associated with eigenvalues smaller than a fixed tolerance $1/\nu_{tol}$.
Analougously we repeat the same process for any edge $\mathcal{E}$. Assuming that the edge $\mathcal{E}$ is shared by $\mathcal{N}_\mathcal{E}$ subdomains, we define as in (7.1),(7.2) and (7.3), for $k \in \mathcal{N}_\mathcal{E}$ the matrices $S_{\mathcal{E}\mathcal{E}}^{(k)}, S_{\mathcal{E}\mathcal{E}}^{(k)}$ and $\widetilde{S}_{\mathcal{E}_\Delta\mathcal{E}_\Delta}^{(k)}$. Then we solve the eigenvalues problem:

$$\Big(\sum_{i\in\mathcal{N}_\mathcal{E}} \widetilde{S}_{\mathcal{E}_\Delta\mathcal{E}_\Delta}^{(i)\,-1}\Big)\psi = \Big(\sum_{i\in\mathcal{N}_\mathcal{E}} S_{\mathcal{E}_\Delta\mathcal{E}_\Delta}^{(i)\,-1}\Big)\psi$$

and we select the elements of the primal space as $(\sum_{i\in\mathcal{N}_\mathcal{E}} \widetilde{S}^{(i)\,-1}_{\mathcal{E}_\Delta\mathcal{E}_\Delta})\Psi$, where Ψ, again is the matrix formed column-wise by those eigenvectors associated with eigenvalues smaller than a fixed tolerance $1/\nu_{tol}$.

We do not provide a proof of the following theorem, and we remand to [25] for further details:

THEOREM 7.1. *Let the dual space satisfy the no-net-flux condition given in (1) and let the average operator preserve subdomain normal fluxes as in (6.3) and (6.4). Then, $M^{-1}S$ is symmetric positive definite on the subspace $\widehat{\mathbf{V}}_{\Gamma,B}\times Q_0$; the minimum eigenvalue is 1, and we can algebraically construct a primal space $\mathbf{V}_\Gamma$ such that:*

$$\kappa_2(M^{-1}S) \leq C\nu_{tol}, \qquad \forall \nu_{tol} \in [1,\infty), \tag{7.5}$$

where C is independent of N, h, and H .

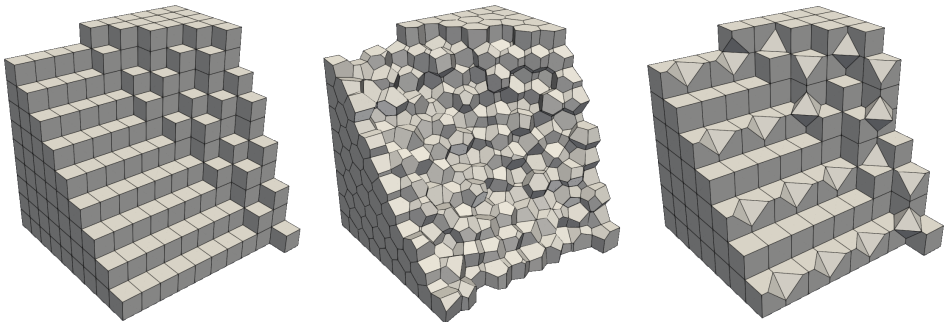

FIG. 1. *Example of CUBE, OCTA and CVT mesh discretization.*

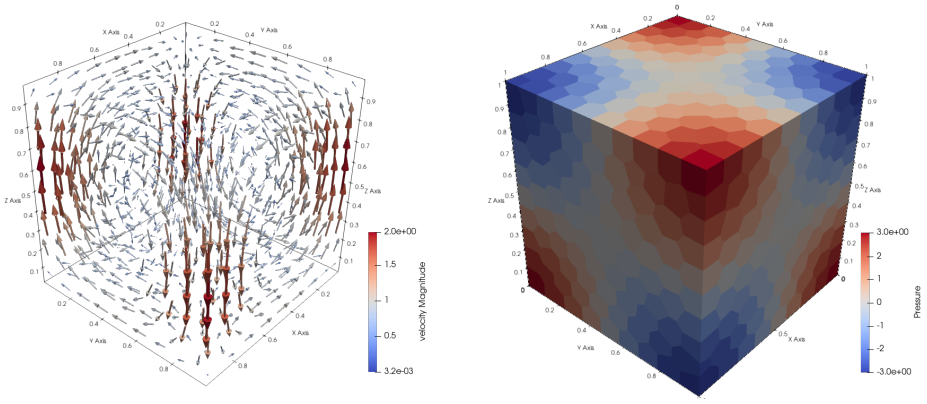

FIG. 2. *3D plot of the solution for the velocity and the pressure for our test case.*

8. Numerical Results. In this Section, we report the numerical results to validate our theoretical estimates of the BDDC algorithm for solving the Stokes model problem (2.5). Unless otherwise stated, we solve a problem on the unit cube $[0,1]^3$

					$\nu_{tol}=2$				$\nu_{tol}=\infty$			
	procs	S^{id}	T_{ass}	S_p	N_Π	it	T_{sol}	S_p	N_Π	it	T_{sol}	S_p
CUBE	4		1 299		447	8	129		4	21	132	
	8	2	871	1.5	1 145	9	46	2.8	21	31	62	2.1
	16	4	418	3.1	2 195	9	29	4.4	51	41	35	3.8
	32	8	202	6.4	4 577	9	12	10.8	125	55	16	8.3
	64	16	105	12.4	7 831	9	5	25.8	311	58	6	22.0
	128	32	53	24.5	13 411	9	4	32.3	643	61	5	26.4
	256	64	27	48.1	22 723	9	5	25.8	1 399	62	5	26.4
CVT	4		2 456		661	9	754		15	38	711	
	8	2	1 423	1.7	1 655	10	334	2.3	130	41	248	2.9
	16	4	816	3.0	3 289	10	157	4.8	337	42	174	4.1
	32	8	400	6.1	6 641	10	61	12.4	905	46	66	10.8
	64	16	216	11.4	10 355	10	21	35.9	2326	33	21	33.9
	128	32	126	19.5	17 566	11	11	68.5	4398	32	9	79.0
	256	64	72	34.1	27 429	11	9	83.8	10 608	32	8	93.2
OCTA	4		3 225		476	8	127		7	26	152	
	8	2	1 637	2.0	1 217	8	50	2.6	21	32	59	2.6
	16	4	838	3.9	2 299	8	30	4.3	51	41	36	4.2
	32	8	434	7.4	4 793	8	12	10.5	125	57	16	9.5
	64	16	218	14.8	8 063	8	5	24.0	311	64	7	21.7
	128	32	116	27.8	14 342	9	6	21.9	643	76	5	30.4
	256	64	56	57.6	26 708	9	5	23.5	1 676	70	7	21.7

TABLE 1

Test 1. Strong Scaling with $k = 2$. Number of elements for CUBE = 13 824 , CVT = 4 000 and OCTA = 15 552.

			$\nu_{tol}=2$			$\nu_{tol}=\infty$		
	nEl	nDofs	N_Π	it	k_2	N_Π	it	k_2
CUBE	4 096	124 195	2 861	9	1.59	125	44	44.67
	8 000	239 763	3 644	9	1.62	152	50	54.53
	13 824	408 243	4 577	9	1.57	125	54	63.98
	21 952	643 387	5 257	9	1.64	152	58	72.37
	32 768	954 947	6 141	9	1.57	125	62	80.63
CVT	125	8 945	1 192	12	2.29	633	22	7.7
	1 000	76 051	3 666	10	2.01	801	32	16.09
	2 000	154 067	5 018	10	1.93	829	40	28.35
	4 000	311 155	6 700	10	1.92	836	46	37.42
	8 000	626 455	8 890	10	1.90	833	56	53.10
OCTA	576	22 035	1 313	9	1.76	125	36	26.15
	4 608	166 179	3 065	8	1.52	125	40	37.19
	9 000	320 763	4 571	9	1.64	157	57	47.31
	15 552	549 939	4 793	8	1.53	125	57	70.78
	30 375	1 065 693	8 513	10	1.85	474	57	46.62

TABLE 2

Test 2. Optimality test with respect to the mesh size, with $k = 2$ and procs = 32.

with a known analytical solution (Figure 2) whose vector velocity field has zero normal component on all the faces of the cube. The PDE we are solving has Neumann boundary conditions on the top and the bottom faces, and homogeneous Dirichlet boundary conditions on the others. The BDDC method is used as a preconditioner for system (4.5), which is solved by the CG method with a stopping criterion of a 10^{-8} reduction of the l^2-norm of the relative residual. We consider three types of meshes: hexahedral (Cube), octahedral (Octa), and Voronoi (CVT), see Figure 1. Our distributed memory implementation is based on the PETSc library [8]. We refer

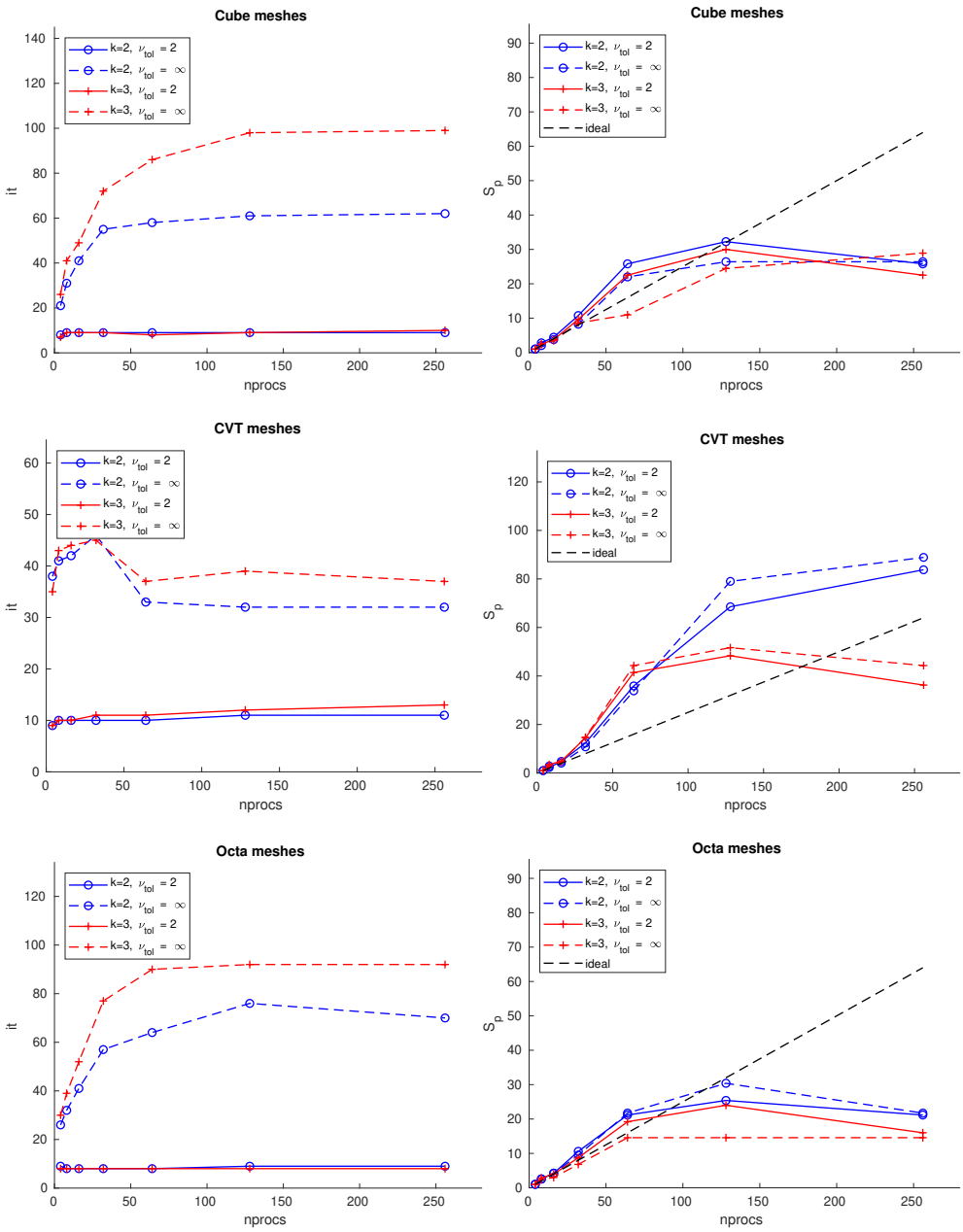

FIG. 3. *Test 1: strong scaling. Iteration of the CG (left) and parallel speedup (right) with the BDDC preconditioners for the two different primal spaces for different meshes and degrees of VEM discretizations.*

to [36] for the details related to the BDDC implementation in PETSc.

In our experiments, we compare two different choices of primal spaces, corresponding to tolerances $\nu_{tol} = 2$ and $\nu_{tol} = \infty$. The first one represents the adaptive coarse space built to keep the condition number under the fixed tolerance $\nu_{tol} = 2$.

	k	nDofs	$\nu_{tol} = 2$ N_Π	it	k_2	$\nu_{tol} = \infty$ N_Π	it	k_2
CUBE	2	16 787	1 273	9	1.81	125	34	23.86
	3	40 667	2 683	8	1.44	125	49	46.34
	4	76 387	4 495	8	1.49	125	64	80.67
CVT	2	8 945	1 192	12	2.29	633	22	7.7
	3	19 256	2 444	12	2.26	633	31	14.89
	4	33 487	4 604	14	3.02	633	46	28.86
OCTA	2	22 035	1 313	9	1.76	125	36	26.15
	3	52 251	2 847	8	1.46	125	55	53.66
	4	96 675	4 951	9	1.61	125	75	91.81

TABLE 3

Test 3. Optimality Test Increasing the polynomial degree k with procs = 32 and number of elements for CUBE = 512, CVT = 125 and OCTA = 576.

	nEl	k	nDofs	MUMPS T_{sol}	Block-Schur it	Block-Schur T_{sol}	Block-Mass it	Block-Mass T_{sol}	BDDC it	BDDC T_{sol}
CUBE	32 768	2	954 947	297	705	110	1809	202	21	26
	13 824	3	1 009 803	416	NC	NC	NC	NC	18	22
	8 000	4	1 119 523	465	NC	NC	NC	NC	13	34
CVT	8 000	2	627 455	913	568	134	1353	277	16	58
	4 000	3	666 301	971	NC	NC	NC	NC	17	103
	2 000	4	571 696	842	NC	NC	NC	NC	22	93
OCTA	30 375	2	1 065 693	285	893	180	2591	381	21	60
	15 552	3	1 322 571	355	NC	NC	NC	NC	19	73
	9 000	4	1 436 523	548	NC	NC	NC	NC	34	97

TABLE 4

Test 4. Solver Comparision. Performance comparision among different parallel solver with procs = 64.

The latter represents the minimal coarse spaces created as explained in Section 4 to satisfy Assumptions 1 and 2. We also compare the BDDC algorithms against our previous block-diagonal preconditioners [23], and the parallel direct solver MUMPS [3, 4]. We conclude by testing the robustness of our adaptive BDDC algorithm on a benchmark problem with variable viscosity. All the numerical tests presented in the following have been performed on the Linux cluster INDACO (www.indaco.unimi.it) of the University of Milan, constituted by 16 nodes, each carrying 2 INTEL XEON E5-2683V4 processors at 2.1 GHz, with 16 cores each.

In the tables we use the following notation: procs = number of CPU cores, nEl = number of VEM elements, k = degree of VEM approximation, nDofs = number of dofs, N_Π = number of primal constraints, it = iteration count (GMRES for Block-Schur and Mass, CG for BDDC), k_2 = conditioning number, T_{ass}= time to assemble the stiffness matrix and the right-hand side, T_{sol} = time to solve the interface saddle point problem and S^{id} = ideal speed up, S_p = parallel speed up.

8.1. Test 1: strong scaling. We first study the strong scalability of our solvers. We keep fixed the global number of dofs and the degree of the VEM approximation k, while we increase the number of processors from 4 to 256. We consider a CUBE mesh with 408 243 dofs, a CVT mesh with 311 155 dofs and an OCTA mesh with 549 939 dofs. Denoting by p the number of processors, the parallel speedup is defined as:

$$S_p := \frac{\text{CPU time with 4 processors}}{\text{CPU time with p processors}}.$$

$DR(\nu)$		$1e+2$		$1e+4$		$1e+6$	
	n	it	k_2	it	k_2	it	k_2
CUBE	1	19	7.7	20	7.6	19	7.7
	5	19	7.7	19	7.6	19	8.4
	10	19	7.6	19	7.6	19	8.5
	20	19	7.4	19	7.7	19	6.1
CVT	1	15	4.8	16	5.2	17	6.1
	5	15	4.8	17	5.8	19	8.1
	10	15	5.1	17	6.1	20	8.1
	20	17	7.7	20	9.7	28	15.2
OCTA	1	19	7.4	19	7.6	20	8.4
	5	18	7.2	19	7.6	19	8.4
	10	18	6.8	20	8.8	19	8.9
	20	18	7.0	19	7.6	18	8.4

		$k=2$			
	ν_{tol}	N_Π	it	k_2	T_{sol}
CUBE	2	9876	17	4.9	7
	10	2657	30	11.7	6
	100	973	77	107.4	9
	∞	311	2003	1.70E+05	285
CVT	2	13054	15	4.0	25
	10	4123	34	14.1	24
	100	2547	78	74.6	31
	∞	2326	166	6.60E+02	48
OCTA	2	10180	11	2.2	7
	10	2463	30	11.3	6
	100	897	66	59.5	9
	∞	311	1906	1.75E+05	287

TABLE 5

Test 5. Multi-sinker benchmark problem with procs = 64 and number of elements for CUBE = 13 824, CVT = 4 000 and OCTA = 15 552. On the left a test increasing the coefficient ratio of the heterogeneity, on the right a test comparing different values for the ν_{tol} of the adaptive coarse space against the minimal one

.

In Table 1, we report the results related to the three polyhedral meshes with $k = 2$. In Figure 3, we plot the number of iterations and the parallel speedup for the case $k = 3$. We observe that the CPU time T_{ass}, needed to assemble the stiffness matrix and the right-hand-side is scalable, with a speedup very close to the ideal ones. The adaptive BDDC method ($\nu_{tol} = 2$) results algorithmically scalable since the number of CG iterations remains bounded and the solution time decreases as the number of the processors increases. The parallel speedup shows a superlinear rate and improves only up to the point where communication times start to dominate, as usual in the strong scaling tests of domain decomposition methods where local problems are solved using direct factorizations. The differences between CUBE, OCTA and CVT meshes are due to the different sparsity patterns of the local subdomain problems. Also, the minimal coarse space results are scalable for the degree $k = 2$ and 3, with the same behavior as the adaptive BDDC.

8.2. Test 2: optimality test with respect to the mesh size. We now perform an optimality test with respect to the mesh size: we keep fixed the number of processors at 32 and the degree of the VEM discretization $k = 2$, and we increase the number of dofs by refining the mesh. The results are reported in Table 2. We observe that the adaptive solver has an optimal behavior irrespective of the type of polyhedral mesh considered since the number of iterations is independent of the refinement level. The minimal coarse space shows a quasi-optimal behavior since both the iteration count and the condition number exhibit a logarithmic growth as predicted by Theorem 4.3. Similar results also occur for the cases $k = 3$ and 4.

8.3. Test 3: optimality test with respect to the polynomial degree. In this test, we study the robustness of our preconditioners when increasing the polynomial degree of the VEM discretization. The tests are performed by keeping fixed the number of processors (32) and the number of elements. The results reported in Table 3 show that the adaptive BDDC algorithm is robust with respect to the polynomial degree in all meshes. The BDDC solver with minimal coarse space instead exhibits a slight increase of the condition number and iterations count when the degree k

increases.

8.4. Test 4: solvers comparison. In Table 4, we compare the performance of the CG method accelerated by the adaptive BDDC preconditioner against the direct solver MUMPS, the GMRES method accelerated by the Block-Schur preconditioner proposed in [24], and preconditioned GMRES by the Block-Mass preconditioner proposed in [28]. The Block-Schur preconditioner is of the form:

$$B = \begin{bmatrix} diag(A)^{-1} & 0 \\ 0 & \widetilde{S}^{-1} \end{bmatrix}$$

where $\widetilde{S} = -Bdiag(A)^{-1}B^T$ is the approximate Schur complement of the system (3.19) and the inversion of this matrix is performed by MUMPS, while the latter substitutes the bottom right block with the mass matrix for the pressure. We can see that the adaptive BDDC is significantly faster than the other solvers for all the meshes considered and for the three different degrees of the VEM discretization. We also note that both the Schur complement based preconditioners are not robust for the degree $k = 3$ and 4, since the GMRES method does not converge (NC in the table).

8.5. Test 5: Multi-sinker benchmark problem. To consider a practical application, as in [35], we conclude by testing the robustness of our adaptive BDDC algorithm on a benchmark problem with heterogeneous viscosity. We perform a multi-sinker test problem with inclusions of equal size placed randomly in the unit cube domain so that they can overlap and intersect the interface among the subdomains. The viscosity coefficient $\nu(\mathbf{x})$ is defined in terms of a C^∞ indicator function $\chi_n(\mathbf{x}) \in [0, 1]$ that accumulates n sinkers via the product of modified Gaussian functions, see [35] for more details about these functions. In this way, the viscosity exhibits sharp gradients, and its dynamic ratio $DR(\nu) := \nu_{max}/\nu_{min}$ in our study can be up to six orders of magnitude. We fix the mesh element size and the number of processes at 64, and we study the iteration count and condition number of the adaptive BDDC algorithm with $\nu_{tol} = 5$, varying the dynamic ratio $DR(\nu)$ from 1 to $1e + 6$, and the number of sinkers n from 1 to 20. The results reported in the left panel of Table 5, obtained on different polyhedral meshes and for a VEM discretization of degree $k = 2$, show the robustness of our adaptive preconditioner since the number of iterations and the condition number are independent of the number of sinkers and the viscosity ratio. We also report a test by varying the tolerance ν_{tol} to highlight the need for an adaptive coarse space in terms of computational timings.

9. Conclusions. We have analyzed BDDC preconditioners for the saddle-point linear system arising from a divergence free VEM discretization of the three-dimensional incompressible Stokes equations. The numerical tests have validated the convergence estimates, showing the scalability and quasi-optimality of the algorithm, under appropriate choices of the coarse space. We have also investigated an adaptive technique to enrich the coarse space, based on deluxe scaling functions, that is more robust than the minimal coarse space with respect to the order of VEM approximation. We have also shown that the adaptive BDDC method outperforms in terms of CPU time other competitive solvers and that it is robust on a challenging multi-sinker test case.

Acknowledgments. We acknowledge the usage of the INDACO Linux Cluster of the University of Milan and the support of INDAM-GNCS.

REFERENCES

[1] R. A. Adams and J. J. Fournier, *Sobolev spaces*, Elsevier, 2003.

[2] B. Ahmad, A. Alsaedi, F. Brezzi, L. D. Marini, and A. Russo, *Equivalent Projectors for Virtual Element Methods*, Computers & Mathematics with Applications, 66 (2013), pp. 376–391.

[3] P. R. Amestoy, I. S. Duff, J.-Y. L'Excellent, and J. Koster, *A fully asynchronous multifrontal solver using distributed dynamic scheduling*, SIAM Journal on Matrix Analysis and Applications, 23 (2001), pp. 15–41.

[4] P. R. Amestoy, A. Guermouche, J.-Y. L'Excellent, and S. Pralet, *Hybrid scheduling for the parallel solution of linear systems*, Parallel computing, 32 (2006), pp. 136–156.

[5] P. F. Antonietti, L. Beirão da Veiga, and G. Manzini, *The Virtual Element Method and its Applications*, Springer International Publishing, 2022.

[6] P. F. Antonietti, S. Berrone, M. Busetto, and M. Verani, *Agglomeration-based geometric multigrid schemes for the Virtual Element Method*, SIAM Journal on Numerical Analysis, 61 (2023), pp. 223–249.

[7] P. F. Antonietti, L. Mascotto, and M. Verani, *A multigrid algorithm for the p-version of the virtual element method*, ESAIM: Math. Model. Numer. Anal., 52 (2018), pp. 337–364.

[8] S. Balay, S. Abhyankar, M. Adams, J. Brown, P. Brune, K. Buschelman, L. Dalcin, A. Dener, V. Eijkhout, W. Gropp, et al., *PETSc users manual*, tech. report, Argonne National Laboratory, 2019.

[9] L. Beirão da Veiga, N. Bellomo, F. Brezzi, and L. D. Marini, *Recent results and perspectives of virtual element methods*, Math. Mod. Meth. Appl. Sci., 31 (2021), pp. 2819–3058.

[10] L. Beirão da Veiga, F. Brezzi, A. Cangiani, G. Manzini, L. D. Marini, and A. Russo, *Basic Principles of Virtual Element Methods*, Math. Mod. Meth. Appl. Sci., 23 (2013), pp. 199–214.

[11] L. Beirão da Veiga, F. Dassi, and G. Vacca, *The Stokes complex for Virtual Elements in three dimensions*, Mathematical Models and Methods in Applied Sciences, 30 (2020), pp. 477–512.

[12] L. Beirão da Veiga, C. Lovadina, and G. Vacca, *Divergence Free Virtual Elements for the Stokes Problem on Polygonal Meshes*, ESAIM: Math. Mod. Numer. Anal., 51 (2017), pp. 509–535.

[13] L. Beirão da Veiga, C. Lovadina, and G. Vacca, *Virtual Elements for the Navier–Stokes Problem on Polygonal Meshes*, SIAM J. Numer. Anal., 56 (2018), pp. 1210–1242.

[14] S. Bertoluzza, M. Pennacchio, and D. Prada, *BDDC and FETI-DP for the virtual element method*, Calcolo, 54 (2017), pp. 1565–1593.

[15] S. Bertoluzza, M. Pennacchio, and D. Prada, *FETI-DP for the Three Dimensional Virtual Element Method*, SIAM J. Numer. Anal., 58 (2020), pp. 1556–1591.

[16] T. Bevilacqua, F. Dassi, S. Zampini, and S. Scacchi, *BDDC preconditioners for virtual element approximations of the three-dimensional Stokes equations*, 2023, https://arxiv.org/abs/2304.09770.

[17] T. Bevilacqua and S. Scacchi, *BDDC preconditioners for divergence free virtual element discretizations of the Stokes equations*, Journal of Scientific Computing, 92 (2022), pp. 1–27.

[18] D. Boffi, F. Brezzi, and M. Fortin, *Mixed finite element methods and applications*, vol. 44, Springer, 2013.

[19] S. C. Brenner and L.-Y. Sung, *Virtual element methods on meshes with small edges or faces*, Mathematical Models and Methods in Applied Sciences, 28 (2018), pp. 1291–1336.

[20] J. G. Calvo, *On the approximation of a virtual coarse space for domain decomposition methods in two dimensions*, Math. Mod. Meth. Appl. Sci., 28 (2018), pp. 1267–1289.

[21] J. G. Calvo, *An overlapping Schwarz method for virtual element discretizations in two dimensions*, Comput. Math. Appl., 77 (2019), pp. 1163–1177.

[22] L. Chen and J. Huang, *Some error analysis on virtual element methods*, Calcolo, 55 (2018), pp. 1–23.

[23] F. Dassi and S. Scacchi, *Parallel block preconditioners for three-dimensional virtual element discretizations of saddle-point problems*, Comput. Meth. Appl. Mech. Eng., 372 (2020), p. 113424.

[24] F. Dassi and S. Scacchi, *Parallel solvers for virtual element discretizations of elliptic equations in mixed form*, Computers & Mathematics with Applications, 79 (2020), pp. 1972–1989.

[25] F. Dassi, S. Zampini, and S. Scacchi, *Robust and scalable adaptive BDDC preconditioners for virtual element discretizations of elliptic partial differential equations in mixed form*,

Comput. Meth. Appl. Mech. Eng., 391 (2022), p. 114620.
[26] C. R. Dohrmann, *A preconditioner for substructuring based on constrained energy minimization*, SIAM Journal on Scientific Computing, 25 (2003), pp. 246–258.
[27] P. Goldfeld, L. F. Pavarino, and O. B. Widlund, *Balancing Neumann-Neumann preconditioners for mixed approximations of heterogeneous problems in linear elasticity*, Numerische Mathematik, 95 (2003), pp. 283–324.
[28] P. P. Grinevich and M. A. Olshanskii, *An iterative method for the stokes-type problem with variable viscosity*, SIAM Journal on Scientific Computing, 31 (2009), pp. 3959–3978.
[29] A. Klawonn, M. Lanser, and A. Wasiak, *Adaptive and Frugal FETI-DP for Virtual Elements*, Vietnam Journal of Mathematics, (2022), pp. 1–23.
[30] A. Klawonn, M. Lanser, and A. Wasiak, *Three-level BDDC for Virtual Elements*, tech. report, Universität zu Köln, 2022.
[31] A. Klawonn and O. B. Widlund, *Dual-primal FETI methods for linear elasticity*, Comm. Pure Appl. Math., 59 (2006), pp. 1523–1572.
[32] A. Klawonn and O. B. Widlund, *Dual-primal FETI methods for linear elasticity*, Communications on Pure and Applied Mathematics: A Journal Issued by the Courant Institute of Mathematical Sciences, 59 (2006), pp. 1523–1572.
[33] J. Li and O. Widlund, *BDDC algorithms for incompressible Stokes equations*, SIAM J. Numer. Anal., 44 (2006), pp. 2432–2455.
[34] L. F. Pavarino and O. B. Widlund, *Balancing Neumann-Neumann methods for incompressible Stokes equations*, Comm. Pure Appl. Math., 55 (2002), pp. 302–335.
[35] J. Rudi, G. Stadler, and O. Ghattas, *Weighted BFBT preconditioner for Stokes flow problems with highly heterogeneous viscosity*, SIAM Journal on Scientific Computing, 39 (2017), pp. S272–S297.
[36] S. Zampini, *PCBDDC: a class of robust dual-primal methods in PETSc*, SIAM Journal on Scientific Computing, 38 (2016), pp. S282–S306.
[37] S. Zampini and X. Tu, *Multilevel balancing domain decomposition by constraints deluxe algorithms with adaptive coarse spaces for flow in porous media*, SIAM Journal on Scientific Computing, 39 (2017), pp. A1389–A1415.